Available online at www.sciencedirect.com
SCIENCE DIRECT®
Pergamon
Cement and Concrete Research 34 (2004) 1591–1598
CEMENT AND CONCRETE RESEARCH

Solution properties of solids in the ettringite—thaumasite solid solution series

Donald E. Macphee[a,*], Stephanie J. Barnett[b]

[a]Department of Chemistry, University of Aberdeen, Meston Walk, Old Aberdeen AB24 3UE, Scotland, UK
[b]Department of Civil Engineering, University of Liverpool, Liverpool, L69 3GQ, UK

Received 2 October 2003; accepted 24 February 2004

Abstract

The thaumasite form of sulfate attack (TSA) has received considerable research attention since its discovery in several motorway bridge foundations in the UK in 1998. Its significance as a deterioration mechanism in concrete, leading to the fluidisation of the matrix in extreme cases, is now acknowledged. Despite the continuing uncertainties that exist with regard to mechanisms for thaumasite formation, there is now reasonable agreement on conditions that favour TSA, and, as with all deleterious reactions affecting concrete structures, there is a desire to be able to anticipate the likelihood of occurrence so that such problems can be 'designed out' in the formulation stage. Inevitably, this points to the development of suitable models and the generation of reliable data. It is towards this latter goal that this paper is focused. Building on our previous studies, which reported on the means of fixing intermediate compositions in the ettringite–thaumasite solid solution series, this paper describes the treatment of solubility data, which can be utilised in phase development and solubility models involving this system.

Keywords: Ettringite–thaumasite; Thermodynamic calculations; Immiscibility; Stability

1. Introduction

There has been much reported recently on the occurrence and properties of thaumasite in concrete[1]. This focus has been, to a large extent, due to the identification of the thaumasite form of sulfate attack (TSA) in a number of UK motorway bridge foundations in the UK in 1998 and the subsequent study and report of the UK government's Thaumasite Expert Group [1]. However, there has since been several reports to indicate that, far from being a UK problem, TSA has been identified in several other countries around the world [2].

TSA is a deterioration mechanism, analogous to conventional sulfate attack, but instead of the formation of ettringite ($C_6A\bar{S}_3H_{32}$) from the reaction between sulfate ions and aluminous components of Portland cement, thaumasite ($C_3S\bar{C}\bar{S}H_{15}$) forms, under suitable conditions, from the reaction between sulfate and carbonate ions and C-S-H gel, the main binding phase in Portland cement concrete. Whilst ettringite formation can lead to expansion and cracking, the loss of C-S-H due to TSA can cause the concrete to lose strength and, in extreme cases, fluidise the matrix. It is an interesting coincidence that these deterioration products are so closely related structurally. This may, in fact, have caused previous cases of TSA to be misdiagnosed as conventional sulfate attack. A further implication of this structural similarity is that ettringite and thaumasite form a partial solid solution with each other, the extent of which has only recently been reported [3,4].

As a consequence of this focus on thaumasite, it is now widely acknowledged that extreme TSA can seriously deteriorate structural concrete. The conditions that promote thaumasite formation in Portland cement concrete are, however, still the subject of debate, but there is reasonable general agreement that lower temperatures and exposure to groundwater sulfates are favourable. When other conditions are right, the source of necessary carbonate may be provided by groundwater carbonates or from limestone aggregates. This is supported by recent thermodynamic calculations on cement systems based on solubility data [5]. This study also

* Corresponding author. Tel.: +44-1224-272941; fax: +44-1224-272921.
E-mail address: d.e.macphee@abdn.ac.uk (D.E. Macphee).

[1] The 1st International Conference on Thaumasite in Cementitious Materials was held at the Building Research Establishment, Garston, UK, in June 2002. The conference featured over 60 papers on topics including fundamental property measurements, laboratory and field studies and impact on building codes.

0008-8846/$ – see front matter © 2004 Elsevier Ltd. All rights reserved.
doi:10.1016/j.cemconres.2004.02.022

concluded that thaumasite stability is generally favoured by higher sulfate concentrations than those which would stabilise ettringite and that thaumasite is stable at lower pH; that is, thaumasite stability regimes exist where ettringite is not a coexisting phase. Furthermore, these calculations indicate that thaumasite, considered to be a low-temperature phase, is stable at temperatures as high as 20 °C.

Several laboratory trials and field studies have shown that the use of supplementary cementitious materials (SCMs), such as blastfurnace slag, can, to some extent, mitigate thaumasite formation. It would seem therefore that, empirically at least, there are means to prevent the deleterious TSA from occurring. It would be much more reassuring, however, if a scientific basis can be established for such protection. Such a basis provides the framework for modelling reaction pathways and equilibrium phase assemblages and consequently offers direction towards durable concrete formulations. However, although such models have yet to be developed, steady progress is being made through the generation of new experimental data. It is in this direction that this paper is focused. The calculations of Damidot et al. [5] acknowledge the significance of solid solutions in the C-S-H [6] and hydrogarnet [7] systems, for which thermodynamic data have already been reported, but solid solutions in the thaumasite–ettringite series have not yet been integrated into solubility models. This paper therefore expands on the previously reported compositional characterisation of solid solutions in this series [3,4] and reports aqueous solubility data for these solids at 5, 15 and 30 °C so that this deficiency in the database can be addressed.

2. Calculations of compositions in the ettringite–thaumasite system

Characterising phase equilibria in the ettringite–thaumasite solid solution series has been complicated by the presence of additional phases arising from the synthesis of solids in the series. Although Aguilera et al. [8] subsequently demonstrated a route to phase pure thaumasite, the procedures adopted here, i.e., based on that of Struble [9] for synthesis of ettringite–thaumasite solid solutions, resulted in impure preparations with C-S-H and calcite [3]. Ref. [3] describes, in detail, the means of analytically 'isolating' the ettringite–thaumasite components of the mixture, and we also describe these briefly here with reference to Figs. 1 and 2. The important constituent of the mixture with respect to the analysis is the octahedrally coordinated silicon (Si_{oct}), found uniquely in the ettringite–thaumasite solid solution. Fourier transform infrared (FTIR) spectroscopy, capable of distinguishing and quantifying Si_{oct} (see Fig. 1), was employed in the analysis, along with quantitative X-ray diffraction (QXRD), which quantifies the ettringite–thaumasite components (Fig. 2). Because Si_{oct} only appears in the ettringite–thaumasite fraction, one can use the FTIR data in combination with QXRD to

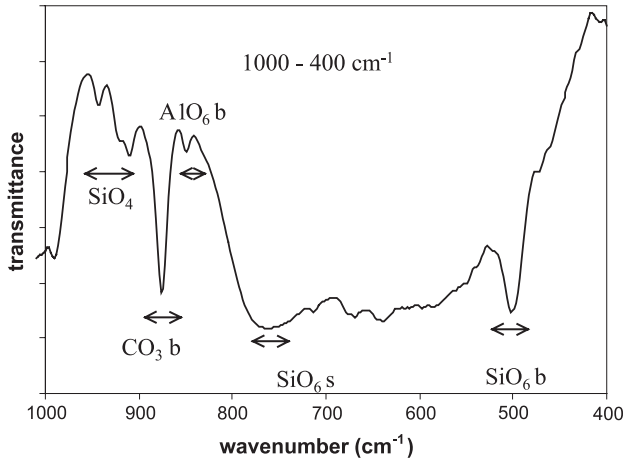

Fig. 1. Partial FTIR spectrum of products obtained in the preparation of solid solutions in the ettringite–thaumasite system. Absorbance assignments indicate stretching (s) or bending (b) vibrations. See Ref. [2] for further details.

derive the molar fraction of Si_{oct} present in the ettringite–thaumasite fraction as follows:

$$n_{Si_{oct}}/\text{mole}(\text{ett}-\text{thaum}) = 2Y \frac{\text{mass}_{std}}{\text{mass}_{ett/thaum}} \frac{\text{MWt}_{ett/thaum}}{\text{MWt}_{std}} \quad (1)$$

where the constant 2 indicates 2 mol of Si/mol of thaumasite (i.e., the formula unit of thaumasite is doubled to be comparable with that of ettringite, which has 2 mol of Al in the octahedral sites). Y is derived from least-squared fitting of the experimental FTIR spectra in the region relevant to Si_{oct} vibration frequencies (475–525 cm^{-1}), with FTIR data calculated from the expression:

$$I_{ci} = X(I_{ei}) + Y(I_{ti}) \quad (2)$$

I_{ci} is the calculated intensity at wavenumber i, I_{ei} and I_{ti} are intensities attributed to ettringite and thaumasite constituents, respectively, at wavenumber i, and X and Y are constants; solutions for X and Y were obtained using Microsoft Solver by minimising the value $\Sigma(I_{ci}-I_{oi})^2$, where I_{oi} is the observed intensity from the experimentally obtained FTIR spectra at wavenumber i. The mass values in Eq. (1) were obtained from QXRD data using the commercial software package Siroquant ([10] or GSAS [11]), and the molecular weight (MWt) ratio was taken as approximately unity. The standard (std) reference material was a high-purity natural thaumasite sample from Crestmore, CA.

Where either a thaumasite- or ettringite-like solid solution is present, the calculated $n_{Si_{oct}}$ is representative of the Si content of that phase. However, when both types of phase are observed, the compositions of the two phases must, at equilibrium, represent the compositions at either end of a miscibility gap in the solid solution series, and an average of two Si contents [$n_{Si_{oct}(avg)}$] is calculated. This provides a means of evaluating the compositions of the solubility limits (n_{ett} and n_{tham}) because the average composition in all of the

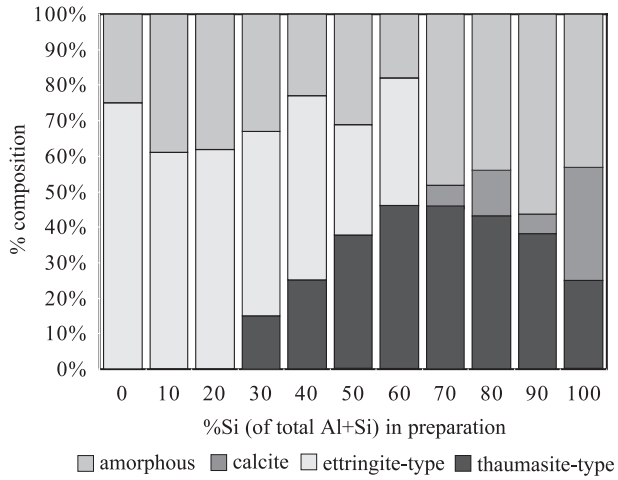

Fig. 2. QXRD data for products obtained in the preparation of solid solutions in the ettringite–thaumasite system. Further details can be found in Ref. [2].

two-phase mixtures is a function of the limiting compositions as follows:

$$n_{\mathrm{Si_{oct}(avg)}} = \frac{\%\mathrm{ett-like}}{100} n_{\mathrm{ett}} + \frac{\%\mathrm{thaum-like}}{100} n_{\mathrm{thaum}} \qquad (3)$$

Where %ett- and %thaum-like can be obtained from QXRD data, and $n_{\mathrm{Si_{oct}(avg)}}$ is calculated from Eq. (1). A least-square method can again be applied. This time, the values of n_{ett} and n_{thaum} are tested by the evaluation of a calculated $[n_{\mathrm{Si_{oct}(avg)}}]_{\mathrm{calc}}$ using Eq. (3), and $\{[n_{\mathrm{Si_{oct}(avg)}}]_{\mathrm{calc}} - [n_{\mathrm{Si_{oct}(avg)}}]_{\mathrm{obs}}\}^2$ is minimised to find a solution for n_{ett} and n_{thaum}, which defines the compositions at the ettringite and thaumasite end of the miscibility gap, respectively.

Our first approach [3] relied on XRD as a means of identifying systems with immiscible phases. However, subsequent work indicated that XRD was not sensitive to small amounts of ettringite (up to 10%) at the thaumasite end of the series [4]. The application of the fitting procedures based on all two-phase mixtures suggested that what appeared to be a single phase, Al-substituted thaumasite by XRD is more likely to be a mixture of two phases, in which the ettringite-like phase concentration is below the XRD detection limit (which is high for ettringite in the presence of substantial amounts of thaumasite). Consequently, the immiscibility gap is calculated to be larger than reported in Ref. [3], ranging from approximately $n_{\mathrm{Si_{oct}}} = 1.0$ at the ettringite end to 1.95 at the thaumasite end. In fact, as thaumasite has $n_{\mathrm{Si_{oct}}} = 2$, our results suggest that the degree of Al substitution in thaumasite, if permitted at all, is small. For further details of these procedures and interpretation, the reader is directed to Refs. [3] and [4].

3. Experimental procedures

As the products from the previous study [3] were also used here, full details of our experimental procedures are already reported [3,4]. Only a brief description is provided here for convenience. Appropriate amounts of a CaO/H_2O slurry, made by mixing previously calcined AnalaR $CaCO_3$ with a 10% sucrose solution in water, and sodium silicate, sodium aluminate, sodium carbonate and sodium sulfate solutions, as necessary to provide a series of solids with variable Si/Al ratios in the range 0–2 (increasing by 10% increments), and CO_3/SO_4 ratios of 1:1 were mixed and sealed into high-density polypropylene bottles. All preparations were carried out under a nitrogen atmosphere, and the solutions were prepared from boiled, deionised water. Each of the 11 preparations was periodically agitated for 6 months at 5 °C. Immediately afterwards, portions of each solid were extracted for X-ray and FTIR analyses (see Refs. [3,4]). Further portions of selected solids were extracted, washed with boiled, deionised water and mixed in three separate smaller bottles with boiled, deionised water. The contents of each bottle were sealed under nitrogen. These bottles were then transferred to water baths at either 5, 15 or 30 °C and periodically shaken over a further 6 months. At various times, aqueous samples were extracted under nitrogen for analysis, and the aqueous phase was carefully replaced with fresh solvent.

Calcium, aluminium, silicon, sulfate and carbonate levels in the solutions were analysed. Calcium was determined by atomic absorption spectroscopy using an air/acetylene flame. Prior to analysis, 2500 ppm K^+ (as KCl) was added to the samples to suppress the ionisation of the Ca atoms in the flame. Aluminium and silicon were measured by spectrophotometry using the Catechol Violet [12] and molybdate blue [13] methods, respectively.

Sulfate and carbonate were determined by ion chromatography using a Dionex DX120 ion chromatograph. For sulfate analysis, the chromatograph was fitted with a Dionex AS14-4-mm ion exchange column (with an AG14-4-mm guard column). The eluent used was 3.5 mM Na_2CO_3/1 mM $NaHCO_3$. The suppression of the eluent conductivity was by an ASRS Ultra self-regenerating suppressor with distilled water regenerant. Carbonate was measured using an ICE-AS1 ion exclusion column with 0.1 mM HCl eluent. An AMMR-II micromembrane suppressor was used with 5 mM tetrabutylammonium hydroxide regenerant.

The experiment was terminated when solution concentrations had established steady-state values, as can be determined by trends, such as are illustrated, e.g., in Fig. 3. At this point, both solid- and aqueous-phase extracts were analysed, with the solids being analysed as described above and in Refs. [3] and [4]. XRD patterns were obtained on a Bruker AX8 diffractometer, using Cu Kα radiation over the range 5°–60° 2θ, with a step size of 0.04° and a count time of 4 s/step. An internal standard (α-Al_2O_3) was interground with the sample in a 1:1 weight ratio, the mixture being side-loaded into the sample holder to minimise preferred orientation. A Nicolet Nexus 870 FTIR transmission instrument was used to collect infrared spectra in the wavenumber

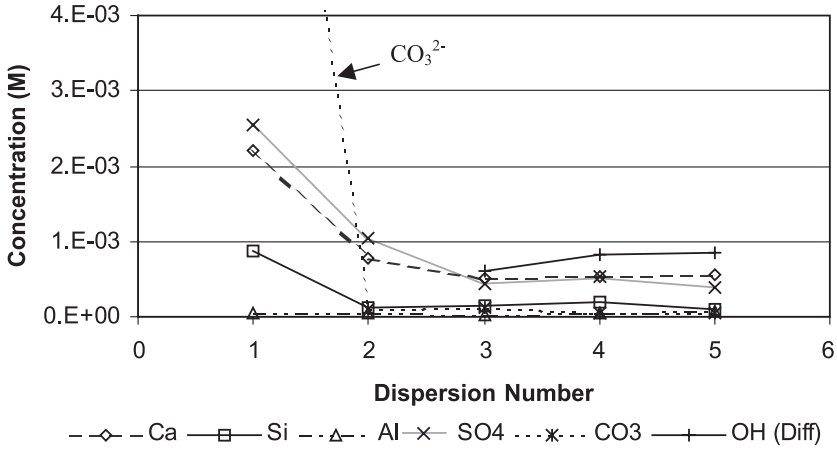

Fig. 3. Example of the variation in aqueous ionic concentrations over solid products as a function of number of redispersions in boiled, deionised water. These data are from the system with target molar Si/Al = 90:10, equilibrated at 5 °C. Steady-state concentrations for each ion were extracted from the level portions of the graph.

range 400–4000 cm^{-1} from accurately known masses of samples interground with dried KBr and pressed into discs at 2000 psi for 5 min.

4. Results and discussion

4.1. Solid analyses

Steady-state solution compositions are reported in Table 1 for all systems (except for thaumasite) at each of the three test temperatures. It should be noted that these solutions are influenced by the presence of impurity phases, which include calcite and C-S-H. The analytical data for thaumasite were not sufficiently precise to include in the Table. Table 2 presents the results of Siroquant/GSAS analyses of QXRD data and shows various distributions of ettringite- and thaumasite-like phases in mixtures with calcite, gypsum and an amorphous phase (C-S-H).

The important link between solid and aqueous phase compositions fundamental to thermodynamic modelling is that they must represent equilibrium mixtures. Thus, the 18 solids collected and analysed at the end of solubility testing are related to the solution compositions in Table 1. Although the FTIR spectra and XRD patterns used for

Table 1
Steady-state aqueous concentrations in solutions above solids prepared to have target compositions intermediate between ettringite and thaumasite

System	Temperature (°C)	[Ca]/M	[Si]/M	[Al]/M	[SO4]/M	[CO3]/M	[OH] /M (calc)	Calc pH
Ettringite	5	1.549e − 03		5.044e − 04	8.944e − 04		8.06e − 04	10.91
Ettringite	15	1.659e − 03		5.207e − 04	9.182e − 04		9.61e − 04	10.98
Ettringite	30	1.814e − 03		7.057e − 04	1.267e − 03		3.88e − 04	10.59
1a80s88	5	1.345e − 03	2.492e − 05	3.206e − 04	4.047e − 04	1.000e − 05	1.51e − 03	11.18
1a80s88	15	1.407e − 03	1.673e − 05	3.695e − 04	4.619e − 04	1.000e − 05	1.48e − 03	11.17
1a80s88	30	2.243e − 03	2.457e − 05	5.863e − 04	6.557e − 04	1.000e − 05	2.54e − 03	11.41
1a50s71	5	1.063e − 03	2.564e − 05	2.498e − 04	3.120e − 04	2.566e − 05	1.18e − 03	11.07
1a50s71	15	1.305e − 03	1.567e − 05	2.794e − 04	5.258e − 04	1.000e − 05	1.24e − 03	11.09
1a50s71	30	1.664e − 03	4.522e − 05	3.358e − 04	5.246e − 04	3.349e − 05	1.83e − 03	11.26
1a20s58	5	6.911e − 04	7.085e − 05	8.895e − 05	2.468e − 04	4.016e − 05	6.48e − 04	10.81
1a20s58	15	8.970e − 04	7.477e − 05	1.338e − 04	2.866e − 04	5.449e − 05	9.03e − 04	10.96
1a20s58	30	6.836e − 04	9.186e − 05	3.206e − 04	4.103e − 04	1.000e − 05	1.14e − 04	10.06
1a10s54	5	5.614e − 04	1.033e − 04	6.078e − 05	3.774e − 04	5.166e − 05	1.01e − 04	10.00
1a10s54	15	8.795e − 04	1.193e − 04	2.046e − 04	5.636e − 04	4.383e − 05	2.20e − 04	10.34
1a10s54	30	1.309e − 03	1.973e − 04	2.027e − 04	6.741e − 04	2.650e − 05	8.16e − 04	10.91

[OH]/M(calc) indicates that hydroxide ion concentrations were calculated from charge balance considerations (i.e., $2[Ca^{2+}]-[Al(OH)_4^-]-[H_3SiO_4^-]-2[SO_4^{2-}]-2[CO_3^{2-}]$). The species identified were taken to be quantitatively the most significant under these aqueous conditions. Data relating to thaumasite are omitted; charge balance calculations returned small but negative values for [OH]/M(calc) at all temperatures, reducing confidence in the analytical data for this system. Target compositions are defined in the column headed "System", in which the sample code has the following significance:

$$1a10 - Si/Al = 90:10;\ 1a20 - Si/Al = 80:20;\ 1a50 - Si/Al = 50:50;\ 1a80 - Si/Al = 20:80$$

Table 2
Distribution of phases in samples recovered from the solubility experiments, as determined by QXRD and $n_{Si_{oct}}$/mol ett–thaum data for the ettringite–thaumasite solid solution component at each of the temperatures studied after repeated dispersion in boiled, deionised water over a period of 6 months

Mole—% Si in preparation	Temperature (°C)	% Thaumasite	% Ettringite	% Calcite	% Gypsum	% Amorphous	$n_{Si_{oct}}$
0 (ettringite)	5	–	70	–	–	30	0.000
	15	–	33	–	2	65	0.000
	30	–	55	–	–	45	0.000
10	5	–	59	–	–	41	0.222
	15	–	43	–	–	57	0.440
	30	–	55	–	–	45	0.161
20 (1A80s88)	5	21	78	–	–	1	0.164
	15	20	50	–	–	30	0.353
	30	9	43	–	–	48	1.004
30	5	24	49	–	–	27	0.892
	15	27	39	–	–	34	1.145
	30	23	47	–	–	30	1.070
40	5	24	39	–	–	37	1.390
	15	30	42	–	–	28	1.120
	30	28	34	–	–	38	1.725
50 (1A50s71)	5	31	37	–	–	32	1.387
	15	35	40	4	–	21	1.126
	30	23	27	–	–	50	1.656
60	5	45	22	trace	–	33	1.660
	15	35	28	–	–	37	1.718
	30	41	29	–	–	30	1.784
70	5	63	10	4	–	23	2.047
	15	54	19	–	–	27	2.046
	30	54	16	–	–	30	2.253
80 (1A20s58)	5	79	–	8	–	13	1.965
	15	35	–	–	–	65	2.233
	30	67	–	–	–	33	2.183
90 (1A10s54)	5	30	–	–	–	70	1.862
	15	72	–	4	–	24	1.933
	30	23	–	–	–	77	2.050
100 (thaumasite)	5	42	–	7	–	51	2.000
	15	18	–	1	–	81	2.000
	30	13	–	1	–	86	2.000

Corresponding solution composition data are available only for those samples identified by bracketed sample codes in the "Mole—% Si in preparation" column.

analysis are not included here, typical data illustrating FTIR and XRD data of these systems can be observed in Fig. 4 of Ref. [4] and Fig. 8 of Ref. [3], respectively. The results of the data analyses for the systems reported here, i.e., the fitting of the FTIR spectra and the incorporation of QXRD data, are also summarised in Table 2, which shows the average compositions, $n_{Si_{oct}(avg)}$, in ettringite–thaumasite solid solutions in the recovered samples.

It may be recalled that where two immiscible constituents of the series are present, the analysis initially provides $n_{Si_{oct}(avg)}$, the average composition of the two phases. The estimated compositions of each phase, representing the limits of the miscibility gap, is obtained by a further fitting procedure using Eq. (3). The results of this analysis are presented in Fig. 4, which highlights the limiting compositions for the system at each of the three temperatures studied; the miscibility gap is represented for each of the three test temperatures by the grey-shaded areas in the figure. It should be noted that the fitting software (Microsoft Excel Solver) was constrained such that $n_{Si_{oct}(avg)}$ could not exceed a value of 2, corresponding to the thaumasite composition. The fitted data, however, are also presented on the graphs as $n_{Si_{oct}(avg)}$ and show a less erratic compositional variation in the two-phase region than from the original $n_{Si_{oct}(avg)}$ data. Within these constraints, the analysis has shown that the compositional range of the miscibility gap is similar at 5 and 15 °C (approximately $\approx 0.72 \leq n_{Si_{oct}} \leq 2.0$) but reduces at 30 °C ($1.2 \leq n_{Si_{oct}} \leq 2.0$). These limits are presented in phase diagram form in Fig. 5. In addition, the immiscibility range observed here is larger at 5 °C than was previously reported [4], with the limit on the ettringite end of the gap extending down to $n_{Si_{oct}} = 0.72$ (compared with approximately 1; [4]). The explanation for this is not yet clear. Although the fitting technique may be subject to some errors in precisely defining limiting compositions, it is not believed that such a large difference could be explained in this way, given that the solutions to the fitting procedure are, by necessity, tested by the degree of fitting. An alternative possibility may be that leaching occurring during the solubility study has brought the system closer to true thermodynamic equilibrium.

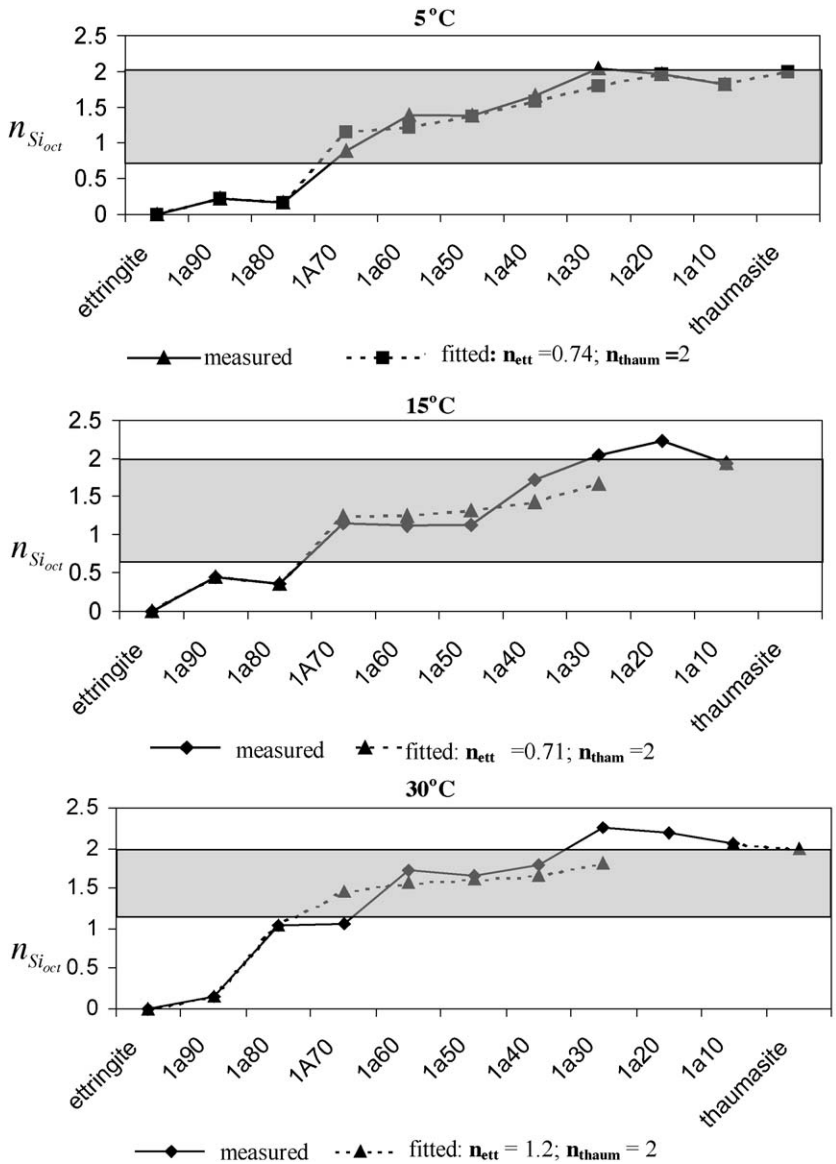

Fig. 4. Results of compositional characterisation of solids following solubility testing at 5, 15 and 30 °C. "Measured" compositions are based on fitting of FTIR data in conjunction with QXRD data, according to Eqs. (1) and (2). "Fitted" data arise from the application of Eq. (3) to all two-phase ettringite–thaumasite mixtures, as distinguished by XRD. n_{ett} and n_{thaum} correspond to compositions ($n_{Si_{oct}}$) at the ettringite and thaumasite ends, respectively, of the miscibility gap (shaded).

4.2. Aqueous solubility characteristics

The solubility of thaumasite may be represented as follows:

$$CaSiO_3.CaSO_4.CaCO_3.15H_2O \leftrightarrow 3Ca^{2+} + H_3SiO_4^- + SO_4^{2-} + CO_3^{2-} + OH^- \quad (4)$$

The identification of the correct ionic species in dissolution equilibria is not critical in the solubility modelling of simple systems, provided that consistency is ensured in the development and subsequent use of constants. The approach taken by PHRQPITZ [14] in Ref. [5] uses a much more rigorous approach. This will be developed elsewhere for these solid solutions. In the first instance, at least, we take a simplistic approach, using concentrations instead of activities of species expected to be the most quantitatively significant, to establish trends.

A solubility product for thaumasite can be defined from Eq. (4):

$$K_{sp(thaum)} = [Ca^{2+}]^3.[H_3SiO_4^-].[SO_4^{2-}].[CO_3^{2-}][OH^-] \quad (5)$$

It is assumed in these calculations that the $[CO_3{}^{2-}]/[SO_4{}^{2-}]$ ratio attributable to thaumasite dissolution is constant at 1, i.e., that thaumasite dissolves congruently.

Similarly, ettringite solubility can be represented as:

$$Ca_6Al_2(SO_4)_3(OH)_{12} \leftrightarrow 6Ca^{2+} + 2Al(OH)_4^- + 3SO_4^{2-} + 4OH^- \quad (6)$$

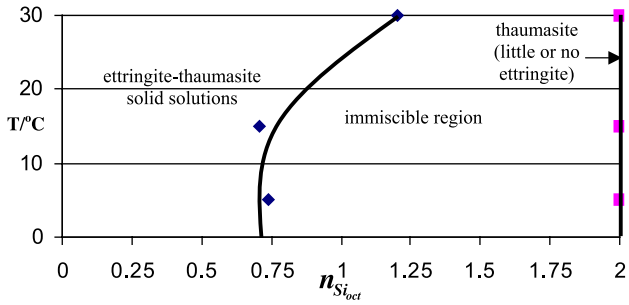

Fig. 5. Partial phase diagram of the ettringite–thaumasite–water system.

and

$$K_{sp(ett)} = [Ca^{2+}]^6.[Al(OH)_4^-]^2.[SO_4^{2-}]^3.[OH^-]^4 \quad (7)$$

If the molar unit of thaumasite in Eq. (4) is doubled, a composite solubility expression for the solid solutions between these end members can be developed:

$$Ca_6Si_{2x}Al_{(2-2x)}(SO_4)_{(3-x)}(CO_3)_{2x}(OH)_{12} \leftrightarrow 6Ca^{2+} + 2xAl(OH)_4^- + (2-2x)H_3SiO_4^- + (x+2)SO_4^{2-} + (2-2x)CO_3^{2-} + (2+2x)OH^- \quad (8)$$

and

$$K_{sp(ett-thaum)} = [Ca^{2+}]^6.[Al(OH)_4^-]^{2x}.[H_3SiO_4^-]^{(2-2x)}.[SO_4^{2-}]^{(x+2)}.[CO_3^{2-}]^{(2-2x)}.[OH^-]^{(2+2x)} \quad (9)$$

The aqueous solution composition data of Table 1 can now be applied in the calculation of $K_{sp(ett-thaum)}$. The value of x is available for each of the solids recovered by interpolation of the $n_{Si_{oct}}$ data from Fig. 4. These are presented, along with K_{sp} and associated indices for Eq. (9) in Table 3. Where $n_{Si_{oct}}$ data indicate compositions out with the miscibility gap, a single K_{sp} is calculated (in these cases, for ettringite or ettringite-like solid solutions). Where compositions within the miscibility gap are indicated, two solubility products are necessary, one for each of the immiscible phases. In these cases, two K_{sp} values are calculated from the same species concentrations but using different stoichiometries (indices in Eq. (9)). It is thus possible, despite the lack of aqueous phase data specific to thaumasite, to determine a K_{sp} value for thaumasite because solid-phase analyses suggests that one of the immiscible solids coexisting at all temperatures has a composition approximating that of thaumasite. The neces-

Table 3
Compositional data ($n_{Si_{oct}}$ and indices) relevant to the calculation of K_{sp}, and K_{sp} data, for solid solutions in the ettringite–thaumasite series

	T/°C	$n_{Si_{oct}}$		Al (%)	$Al(OH)_4$ index	H_3SiO_4 index	SO_4 index	CO_3 index	OH index	$Lg K_{sp}$ [a]
Ettringite	5	0		100	2	0	3	0	4	−44.97
1a80s88	5	0.163		92	1.836	0.163	2.918	0.163	3.836	−45.93
1a50s71	5	0.736		63	1.264	0.736	2.632	0.736	3.264	−47.94
			2	0	0	2	2	2	2	*−49.08*
1a20s58	5	0.736		63	1.264	0.736	2.632	0.736	3.264	−50.27
			2	0	0	2	2	2	2	*−49.65*
1a10s54	5	0.736		63	1.264	0.736	2.632	0.736	3.264	−52.98
			2	0	0	2	2	2	2	*−50.89*
Thaumasite	5	2		0	0	2	2	2	2	
Ettringite	15	0		100	2	0	3	0	4	−44.43
1a80s88	15	0.353		82	1.647	0.353	2.823	0.353	3.647	−45.95
1a50s71	15	0.71		65	1.29	0.71	2.645	0.71	3.29	−47.08
			2	0	0	2	2	2	2	*−49.29*
1a20s58	15									
1a10s54	15	0.71		65	1.29	0.71	2.645	0.71	3.29	−49.60
			2	0	0	2	2	2	2	*−48.71*
Thaumasite	15	2		0	0	2	2	2	2	
Ettringite	30	0		100	2	0	3	0	4	−45.09
1a80s88	30	1.044		48	0.956	1.044	2.478	1.044	2.956	−44.57
1a50s71	30	1.2		40	0.8	1.2	2.4	1.2	2.8	−45.57
			2	0	0	2	2	2	2	*−46.35*
1a20s58	30									−18.99
1a10s54	30	1.2		40	0.8	1.2	2.4	1.2	2.8	−46.45
			2	0	0	2	2	2	2	*−46.38*
Thaumasite	30	2		0	0	2	2	2	2	

[a] Where two values of $n_{Si_{oct}}$ are indicated, two K_{sp} values are necessary (one for each compatible solid of different composition). The first and second K_{sp} values quoted for a given composition at any temperature correspond to the ettringite- and thaumasite-like phases, respectively, at the ettringite and thaumasite limits of the miscibility gap. Although the data specifically for thaumasite are absent (see Table 1), K_{sp} calculations for thaumasite are still possible, as solid analyses indicate that the thaumasite composition approximately represents one of the limits of the miscibility gap at each temperature (such results are shown in italic font).

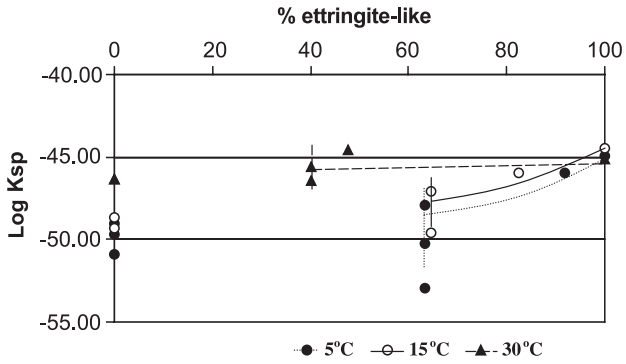

Fig. 6. $K_{sp(ett-thaum)}$ data for solid solutions in the ettringite–thaumasite series at 5, 15 and 30 °C. Solid solutions are apparent only towards the ettringite end of the series.

sary aqueous phase information for the calculation is thus available from these two-phase systems. K_{sp} data for thaumasite evaluated by this route are highlighted in Table 3.

K_{sp} data are summarised in Fig. 6. Despite some scatter in a few (three) data points at 5 °C and 15 °C, representing samples with compositions considered to be on the ettringite limit of the miscibility gap, the temperature dependence of solubility is clearly shown. The range of K_{sp} values at the thaumasite end of the series is broader than at the ettringite end. The interpretation of the behaviour between the end members is complicated by the scatter in data, but there does appear to be a gradual variation in solubilities over the intermediate compositions to the limits of solid solubility.

5. Conclusions

Solid and aqueous phases from a series of preparations intended to give intermediate solid compositions in the incomplete system of ettringite–thaumasite solid solutions have been fully characterised. The results have indicated the following conclusions:

- A miscibility gap in the ettringite–thaumasite system is evident at 5, 15 and 30 °C.
- The compositional range of immiscibility is similar at 5 and 15 °C ($\approx 0.72 \leq n_{Si_{oct}} \leq 2.0$) but smaller at 30 °C ($1.2 \leq n_{Si_{oct}} \leq 2.0$), allowing the construction of a partial phase diagram for the system (Fig. 5).
- The 5 °C data from the present study on leached solids indicate a larger range of immiscibility to that previously reported [4].
- Solubility product expressions for the solid solutions have been developed and used to calculate $K_{sp\ (ett-thaum)}$ for end member as well as intermediate, solid solution phases in the ettringite–thaumasite system.
- Lowest K_{sp} values are obtained at 5 °C.
- Calculated K_{sp} data show temperature dependence in the form of a family of curves. With the exception of a small number of data points, the concentration solubility products appear to vary smoothly across the composition range within the limits of solid miscibility.

Acknowledgements

The authors gratefully acknowledge support from the Engineering and Physical Sciences Research Council (Grant GR/M37714). We are also grateful to Prof. F.P. Glasser for his helpful comments.

References

[1] Report of the Thaumasite Expert Group, The Thaumasite Form of Sulfate Attack: Risks, Diagnosis, Remedial Works and Guidance on New Construction, Her Majesty's Stationary Office, London, 1999.
[2] Proc. 1st International Conference on Thaumasite in Cementitious Materials, Garston, Watford, UK. ISBN 1 86081 557X, (2002 June).
[3] S.J. Barnett, D.E. Macphee, E.E. Lachowski, N.J. Crammond, XRD, EDX and IR analyses of solid solutions between thaumasite and ettringite, Cem. Concr. Res. 32 (2002) 719–730.
[4] S.J. Barnett, D.E. Macphee, N.J. Crammond, Extent of immiscibility in the ettringite–thaumasite system, Cem. Concr. Compos. 25 (2003) 851–855.
[5] D. Damidot, S.J. Barnett, F.P. Glasser, D.E. Macphee, Investigation of the $CaO-Al_2O_3-SiO_2-CaSO_4-CaCO_3-H_2O$ system at 25 °C by thermodynamic calculations, Advances in Cements Research (2004) (in press).
[6] D. Damidot, F.P. Glasser, Investigation of the $CaO-Al_2O_3-SiO_2-H_2O$ system at 25 °C by thermodynamic calculations, Cem. Concr. Res. 25 (1995) 22–28.
[7] T.G. Jappy, F.P. Glasser, Synthesis and stability of silica substituted hydrogarnet, $Ca_3Al_2Si_{3-x}O_{12-4x}(OH)_{4x}$, Adv. Cem. Res. 4 (1991) 1–8.
[8] J. Aguilera, M.T. Blanco-Varella, T. Vázquez, Synthesis of thaumasite, Proc. 1st International Conference on Thaumasite in Cementitious Materials, Garston, Watford, UK. 2002 (June) (ISBN 1 86081 557X).
[9] L.J. Struble, Synthesis and characterisation of ettringite and related phases, Proc. VIIIth Int. Cong. Chem. Cem., 1987, pp. 582–588, Rio de Janeiro.
[10] http://www.ccp14.ac.uk/ccp/web-mirrors/commercial/siroquant/siroqnt/online.htm.
[11] A.C. Larson, R.B. Von Dreele, General structure analysis system (GSAS), Los Alamos Natl. Lab. Rep. LAUR, (2000) 86–748.
[12] W.K. Dougan, A.L. Wilson, The absorptiometric determination of aluminium in water. A comparison of some chromogenic reagents and the development of an improved method, Analyst 99 (1974) 413–430.
[13] R. Ramachandran, P.K. Gupta, An improved spectrophotometric determination of silicate in water based on molybdenum blue, Anal. Chim. Acta 172 (1985) 307–311.
[14] L.N. Plummer, D.L. Parkhurst, G.W. Fleming, S.A. Dunkle, A computer program incorporating Pitzer's equations for calculation of geochemical reactions in brines: US Geological Survey, Water-Resour. Invest. Rep. 99-4153 310 (1988) (US Geological Survey).